Depositing fullerenes in swollen polymer layers via sequential processing of organic solar cells

Depositing Fullerenes in Swollen Polymer Layers via Sequential Processing of Organic Solar Cells

Jacobus J. van Franeker, Sandra Kouijzer, Xianwen Lou, Mathieu Turbiez, Martijn M. Wienk, and René A. J. Janssen**

Polymer solar cells are conventionally processed by coating a multicomponent mixture containing polymer, fullerene, solvent, and cosolvent. The photovoltaic performance strongly depends on the nanoscale morphology of the blend, which is largely determined by the precise nature of the solvent composition and drying conditions. Here, an alternative processing route is investigated in which the two active layer components are deposited sequentially via spin coating or doctor blading. Spin coating the fullerene from *o*-dichlorobenzene on top of the polymer provides virtually identical morphologies and photovoltaic performance. Using blade coating, the influence of the second-layer solvent for the fullerene derivative is investigated in further detail. Different aromatic solvents are compared regarding swelling of the polymer layer, fullerene solubility, and evaporation rate. It is found that while swelling of the polymer by the second-layer solvent is a necessity for sequential processing, the solubility of the fullerene derivative in this solvent has the strongest influence on solar cell performance. Homogeneous layers in which a sufficient amount of fullerene can infiltrate the polymer film can only be achieved when solvents are used that have a very high solubility for the fullerene and swell the polymer layer.

1. Introduction

Organic photovoltaics (OPV) form a promising renewable energy technology. Recently, the efficiency of OPV has increased considerably, now reaching over 10% for polymer:fullerene based solar cells.[1] Also, studies on degradation mechanisms assist in developing devices with increased stability.[2] Ink-based printing of efficient OPV cells is envisioned for large area applications.[3]

Presently, the universal method for manufacturing polymer:fullerene organic solar cells is depositing both components from a common solution. The solution, or ink, thus consists of at least three components: polymer, fullerene, and solvent. To obtain optimized performance it is often mandatory to include cosolvents or processing agents.[4] During film formation the volatile solvents evaporate and the system eventually reaches a state in which it becomes thermodynamically unstable, either because the solubility limit for one of the components is surpassed[5] or because liquid–liquid phase separation occurs when the system enters the spinodal regime.[6] At this point, polymer-rich and fullerene-rich phases will start to form. The growth of these phases is frozen-in when the film solidifies at the time that all solvent has evaporated. The resulting morphology is called a bulk heterojunction.[7] The exact composition of the phases and the typical length scales in this bulk heterojunction morphology are very important for the efficiency of the solar cell.

An alternative processing route is to sequentially deposit layers. This involves depositing the polymer in a first step, followed by the deposition of a fullerene derivative in a second step, using different solvents for each component. In some cases bilayered structures are formed using sequential deposition method, but it is also possible that significant intermixing between the two components takes place.[8] Using this route, it is necessary to use an orthogonal solvent in the second step to avoid washing off the underlying layer, or to use a cross-linked polymer.[9] For sequentially processed poly(3-hexylthiophene):[6,6]phenyl-C_{61}-butyric acid methyl ester (P3HT:[60]PCBM) solar cells thermal annealing is required to achieve proper intermixing of the layers and good solar cell performance.[8,9] For more recent and more efficient polymer:fullerene blends, however, it has been shown that sequential processing of efficient bulk heterojunction solar cells is possible with less or no thermal annealing.[10]

The success of sequential processing hinges on the nature of the orthogonal or selective solvent used to deposit the fullerene,[10] but a detailed understanding of the favorable

J. J. van Franeker, Dr. S. Kouijzer, Dr. X. Lou, Dr. M. M. Wienk, Prof. R. A. J. Janssen
Molecular Materials and Nanosystems & Institute for Complex Molecular Systems
Eindhoven University of Technology
P. O. Box 513, 5600 MB, Eindhoven, The Netherlands
E-mail: j.j.v.franeker@tue.nl; r.a.j.janssen@tue.nl
J. J. van Franeker
Dutch Polymer Institute (DPI)
P. O. Box 902, 5600 AX, Eindhoven, The Netherlands
Dr. M. Turbiez
BASF Schweiz AG
Schwarzwaldallee 215, 4002 Basel, Switzerland
Dr. M. M. Wienk, Prof. R. A. J. Janssen
Dutch Institute for Fundamental Energy Research
De Zaale 20, 5612 AJ, Eindhoven, The Netherlands

DOI: 10.1002/aenm.201500464

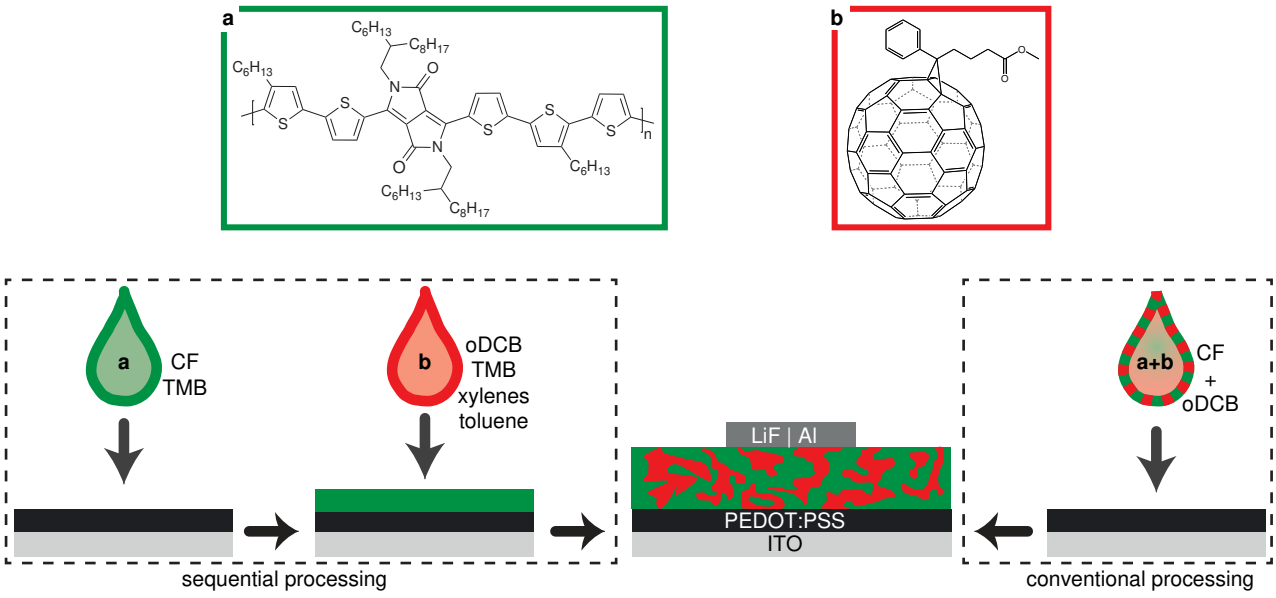

Figure 1. a) Molecular structures of PDPP5T, b) [70]PCBM, and a schematic outline of device processing procedures.

properties and determining characteristics of such a solvent is lacking. Because a substantial intermixing of polymer and fullerene is required for high photovoltaic performance, swelling of the polymer layer by the second solvent has been suggested to be essential.[10d,f] To obtain insight in the parameters controlling the formation of bulk heterojunction formation via sequential processing, we study deposition of [6,6]phenyl-C_{71}-butyric acid methyl ester ([70]PCBM) on top of a poly(diketopyrrolopyrrole–*alt*–quinquethiophene) (PDPP5T) donor polymer film (**Figure 1**) via spin coating and doctor blading. The photovoltaic performance varies widely with the solvent used for depositing [70]PCBM, but for selected solvents sequential processing results in very similar efficiencies and morphologies as conventional one-step processing. We investigate different aromatic solvents with respect to swelling of the PDPP5T layer, evaporation rate, and solubility of the fullerene. Although swelling of the polymer by the second solvent is essential, we demonstrate that the crucial parameter for a high efficiency in sequential layer deposition is the solubility of [70]PCBM in the second solvent. We show that sequential deposition can possibly eliminate the use of chlorinated solvents that are commonly employed in direct, single-step processing protocols for organic solar cells.

2. Results

Conventional processing of optimized PDPP5T:[70]PCBM photoactive blends involves spin coating from chloroform (CF) as a primary solvent with 5 vol% *o*-dichlorobenzene (oDCB) as cosolvent (Figure 1). Blends processed from this CF:oDCB (95:5 v/v) solvent mixture provide power conversion efficiencies (PCEs) of 5.7% (**Table 1**) in solar cells when sandwiched between a transparent ITO/PEDOT:PSS hole collecting electrode and a LiF/Al electron extracting contact.

2.1. Polymer:Fullerene Ratio

For sequential processing we chose to first spin coat a layer of PDPP5T from CF, followed by spin coating [70]PCBM on top (see schematic in Figure 1). The choice of the solvent for depositing [70]PCBM is important. To enable infiltration of [70]PCBM into the previously deposited PDPP5T film, the solvent used for depositing [70]PCBM must have some affinity for PDPP5T. We find that oDCB is such a partial solvent for PDPP5T. After repetitive spin coating of pure oDCB on top of a PDPP5T layer, more than half of the volume of polymer is left behind, even though some is flushed away. Size exclusion chromatography (SEC) (in superheated chloroform, for more details see Supporting Information) of the original polymer (M_p = 29 kDa), a flushed polymer layer (M_p = 32 kDa), and the fraction that dissolved in oDCB (M_p = 5 kDa) revealed that only the low-molecular-weight fraction is flushed away. This makes oDCB a suitable solvent for sequential processing of [70]PCBM on PDPP5T.

First, the delay time between the application of [70]PCBM and the start of spin coating was investigated (Section 2, Supporting Information). Surprisingly, the effect of delay time was

Table 1. Comparison of device performance for the solar cells shown in Figure 3.

Solvent	Ratio[a)]	*d* [nm]	J_{sc}[b)] [mA cm^{-2}]	V_{oc} [V]	FF [%]	PCE [%]
CF only	1:2	92	4.4	0.65	59	1.7
CF:oDCB[c)]	1:2	81	15.5	0.57	65	5.7
CF/oDCB[c)]	1:4	93	13.8	0.55	67	5.0
CF/*o*-xylene[c)]	1:2	90	12.5	0.57	54	3.8

[a)]PDPP5T:[70]PCBM mass ratio; [b)]Calculated by integrating the EQE with AM1.5 solar spectrum; [c)]The ":" sign is used to indicate a solvent mixture, and the "/" sign to indicate sequential processing by the solvents.

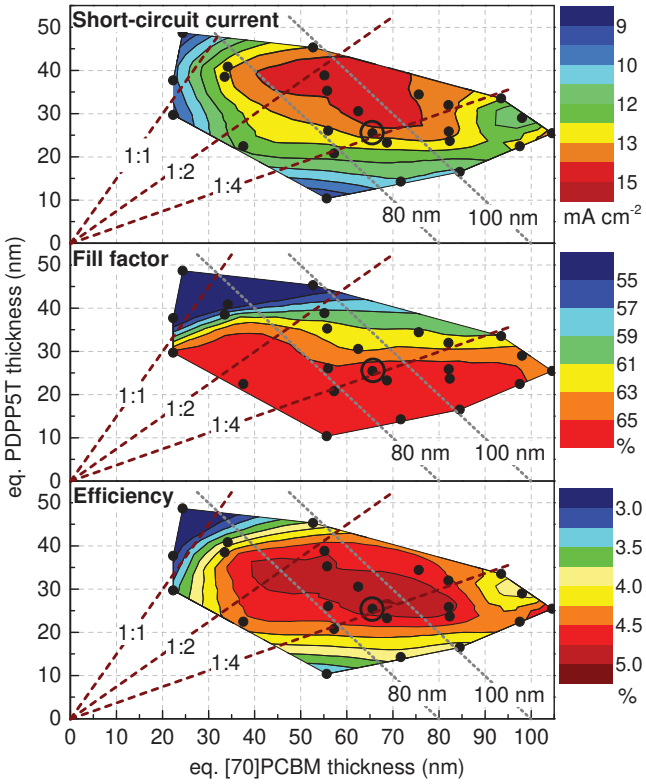

Figure 2. Short-circuit current density, fill factor, and efficiency of PDPP5T:[70]PCBM solar cells prepared via sequential processing as function of PDPP5T and [70]PCBM content (expressed in equivalent layer thicknesses). Black dots indicate actual measurements with the interpolated contours. Brown dashed lines are a guide to the eye for constant PDPP5T:[70]PCBM ratios (1:1, 1:2, and 1:4 w/w) and dotted gray lines are lines of constant total thickness (80 and 100 nm). Parameters for the cell indicated with a circle are collected in Table 1. For these solar cells both layers are spin coated. The J_{sc} and PCE values are from the *J–V* characteristic under simulated AM1.5G white light and are not corrected by integrating the EQE with the AM1.5G spectrum.

very small, which indicates polymer swelling is relatively fast. As the effect was small, in the following the delay was always kept below 5 s.

By depositing PDPP5T from CF at different spin rates and depositing [70]PCBM on top from oDCB also at different spin rates, solar cells with varying PDPP5T:[70]PCBM composition were obtained. The fact that some polymer is washed away in the second spin coating step prevents direct determination of the PDPP5T:[70]PCBM ratio in the film from the increase in film thickness. To measure this ratio, the active layers were redissolved in chloroform and UV–vis absorption spectra of these solutions were fitted with absorption spectra of reference solutions of PDPP5T and [70]PCBM to determine the blend ratio.[11] The total thickness was measured using profilometry. Combining the photovoltaic performance with these data gives insight in the dependence of the various performance parameters on the equivalent layer thicknesses of both components in the total layer, as shown in **Figure 2**. In general, the short-circuit current density (J_{sc}) of polymer:fullerene solar cell strongly depends on the morphology, which influences the efficiency of charge generation, separation, and collection, and on the total layer thickness which influences absorption and charge recombination. For equivalent layer thicknesses of PDPP5T of 20–40 nm, a wide range (40–80 nm) of equivalent [70]PCBM-thicknesses give adequate J_{sc}, fill factor (FF), and PCE (Figure 2). The variation in open-circuit voltage (V_{oc}) was small and is not shown.

2.2. Comparison of Conventional Processing to Sequential Processing

The performance of the best sequentially processed solar cell (CF/oDCB with PDPP5T:[70]PCBM weight ratio of 1:4) is compared with the performance of the optimized bulk heterojunction solar cell (weight ratio of 1:2) fabricated using the CF:oDCB (95:5 v/v) solvent-cosolvent mixture and a device processed without cosolvent (CF-only) in **Figure 3**a,b and Table 1. The external quantum efficiency (EQE) measurement shows that the sequentially processed cell generates a lower photocurrent than the optimized conventionally processed cell. The current density–voltage (*J–V*) measurements show that the open-circuit voltage is also slightly lower, but due to the higher fill factor the PCE is only slightly lower. The PCE of the sequentially processed device is much higher than for the conventionally processed CF-only device.

To visually compare the morphologies that result from the different deposition methods, transmission electron microscope (TEM) images have been acquired for all processing routes (Figure 3c). Narrow polymer fibers can be seen in the TEM images for all films except the CF-only blend. For the CF-only blend the coarse phase separation, with [70]PCBM droplet-like domains that originate from spinodal liquid–liquid decomposition, is detrimental for the device performance.[6] The differences in TEM images of the other processing routes are too small to be conclusive. This indicates that the morphology formed by sequential processing does not differ significantly from the conventional bulk heterojunction, at least within the resolution limits of these TEM images. Vertical composition profiles were obtained by depth-profiling X-ray photoelectron spectroscopy (XPS) (Figure 3d, see Supporting Information for more details). For the conventional single-step spin coating methods the [70]PCBM:PDPP5T ratio is virtually constant. For the sequentially processed PDPP5T:[70]PCBM layer, the average [70]PCBM:PDPP5T ratio determined by XPS is 1:4.5 and the depth profile shows that the PDPP5T and [70]PCBM are well intermixed throughout the device. The apparent increase of the [70]PCBM concentration near the bottom and decrease at the top (Figure 3d) are possibly influenced by the use of the silicon substrate instead of PEDOT:PSS and surface oxidation.

2.3. Processing the Fullerene Derivative from Other Solvents

We also tested sequential processing of [70]PCBM using *o*-xylene instead of oDCB. Nonhalogenated solvents are environmentally friendlier and desired in up-scaling of printing processes for polymer solar cells. A solar cell produced by spin coating PDPP5T from CF, followed by spin coating of [70]PCBM from *o*-xylene gives an optimum PCE of 3.8% (Table 1,

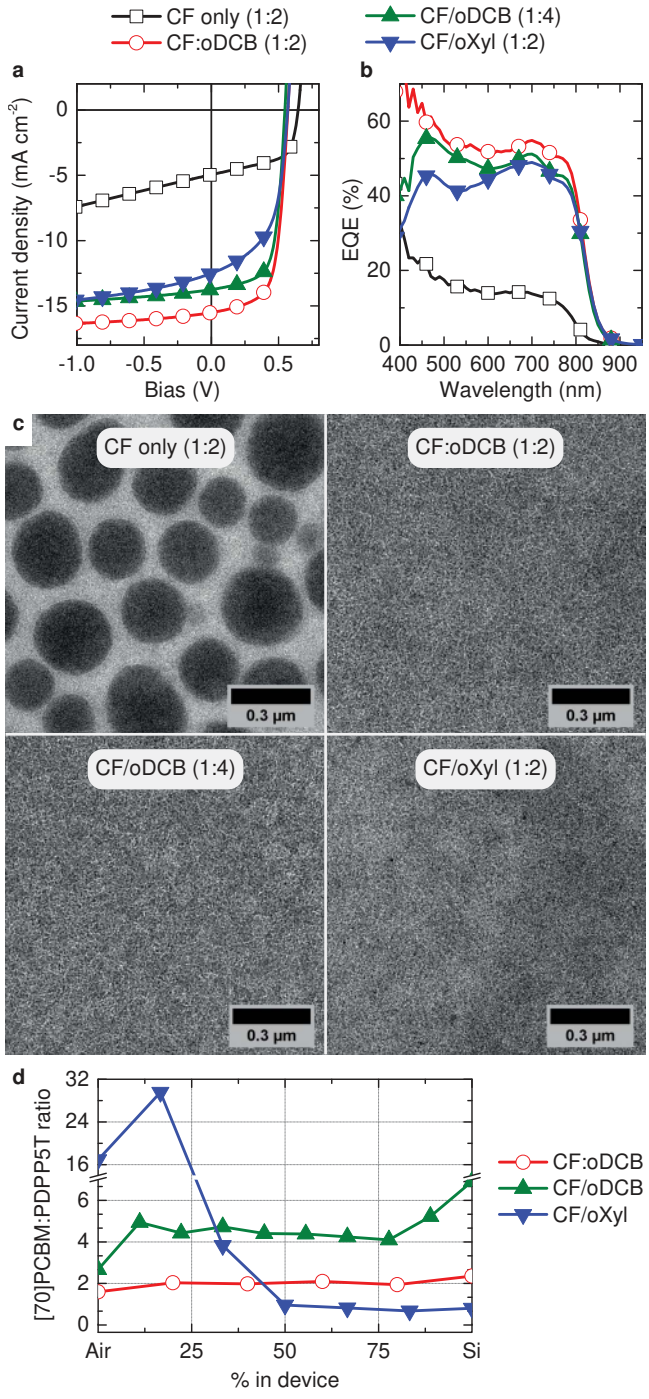

Figure 3. Spin coated solar cells. a) *J–V* and b) EQE measurements of PDPP5T:[70]PCBM (1:2 w/w) solar cells one-step spin coated from CF and from CF:oDCB compared to sequentially spin-coated devices using CF/oDCB (PDPP5T:[70]PCBM ratio 1:4) and CF/*o*-xylene (PDPP5T:[70]PCBM ratio 1:2). c) TEM images (1.21 µm × 1.21 µm) of these films. d) For the latter three processing routes samples have been made on silicon substrates and the depth profile of the [70]PCBM:PDPP5T ratio obtained by XPS is shown.

Figure 3), showing that results are sub-optimal. This is attributed to the formation of a quasi-bilayered structure, as inferred from depth-profiling XPS (Figure 3d). A fullerene-rich phase

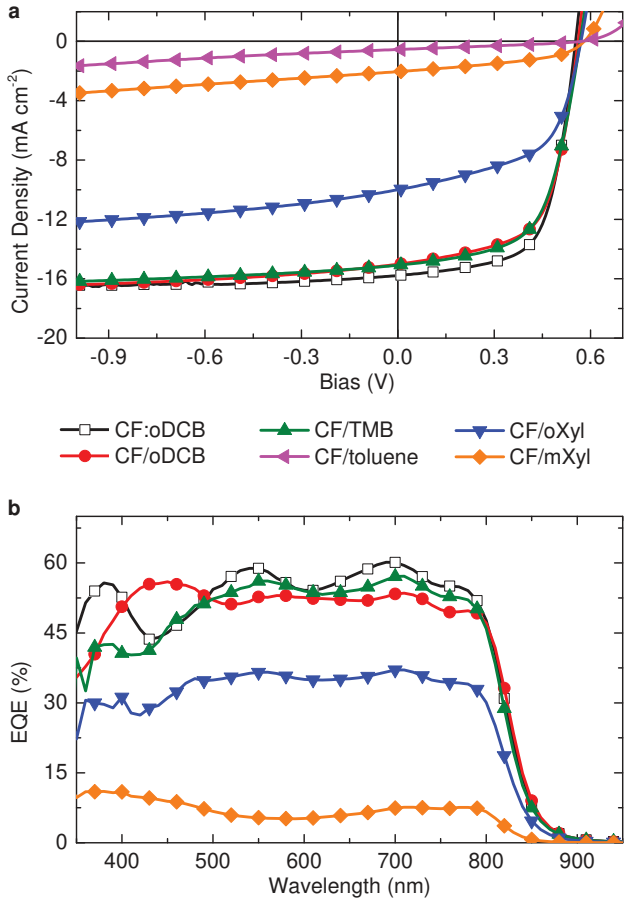

Figure 4. Doctor bladed solar cells. a) *J–V* and b) EQE measurements. The cell labeled CF:oDCB was doctor bladed from a four-component blend in which PDPP5T and [70]PCBM were dissolved in a 1:2 weight ratio in chloroform with 5 vol% oDCB as cosolvent. The other four cells are based on a 40–50 nm thick PDPP5T layer, spin coated from chloroform with a [70]PCBM layer doctor bladed on top from TMB, oDCB, *o*-xylene, *m*-xylene, or toluene.

near the air interface can be beneficial for performance,[12] but the PDPP5T:[70]PCBM ratio of 1:1 in the mixed phase is too low and explains the low fill factor. The results obtained with depositing [70]PCBM from *o*-xylene reveal that the nature of the second solvent is important for the resulting solar cell performance. Using spin coating from *o*-xylene, we found a considerable variation in performance between different runs. Using doctor blading as alternative deposition method for the second-layer turned out to be reproducible and is used in the following.

2.4. Doctor Bladed Solar Cells

Doctor blading is more easily translated to industrially relevant roll-to-roll processes and has been shown to allow for efficient devices for PDPP5T:[70]PCBM blends.[13] As a new reference for conventional doctor blade processing, we processed PDPP5T:[70]PCBM from the CF:oDCB (95:5 v/v) solvent-cosolvent mixture (**Figure 4**). The V_{oc} of 0.55 V is slightly lower than for the spin coated cell (Table 1), but the FF of 65%

Table 2. Solvent properties and solar cells characteristics for sequentially processed solar cells via doctor blading.

Solvent for [70]PCBM[a)]	PDPP5T swelling [mg m^{-2}]	Boiling point[b)] [°C]	[70]PCBM solubility [mg mL^{-1}]	J_{sc}[c)] [mA cm^{-2}]	V_{oc} [V]	FF [%]	PCE [%]
toluene	54	110	50	0.53	0.58	31	0.1
ethylbenzene	47	136	44	0.87	0.58	35	0.2
propylbenzene	48	159	25	1.35	0.58	44	0.3
p-xylene	54	138	12	–	–	–	–
xylenes[d)] (3:1)	–	–	33	2.63	0.59	42	0.7
m-xylene	55	139	101	2.04	0.58	43	0.5
xylenes[d)] (2:3)	–	–	125	4.47	0.58	55	1.4
o-xylene	58	144	229[e)]	10.0	0.57	56	3.2
TMB	56	169	224[e)]	15.1	0.57	61	5.3
oDCB	91[f)]	180	203[g)]	13.8	0.57	63	5.2

[a)]The first PDPP5T layer was spin coated from chloroform and [70]PCBM was applied on top by doctor blading; [b)]Ref. [14]; [c)]Calculated by integrating EQE with AM1.5 solar spectrum; [d)]A mixture of *p*-xylene and *o*-xylene in the indicated ratio; [e)]Close to measurement limit; [f)]Likely to be underestimated, see Section 3, Supporting Information; [g)]Ref. [15].

is the same and the J_{sc} of 15.8 mA cm^{-2} is even slightly higher, which leads to a PCE of 5.7%, which is very similar to the PCE of the spin coated cell. Similar PCEs can be obtained by sequential processing of the second layer either via doctor blading and spin coating. The first (PDPP5T) layer was processed by spin coating from chloroform resulting in a polymer layer thickness of 40–50 nm, but the second ([70]PCBM) layer was deposited by doctor blading, using oDCB as solvent. In this way, a PCE of 5.2% is obtained by sequential processing (Figure 4 and **Table 2**). This is slightly higher than the results when using two spin coated layers (Table 1).

In Figure 4 and Table 2, we show that 1,2,4-trimethylbenzene (TMB) can be used to reach high PCEs of up to 5.3%, similar to that reached by oDCB. Again, with *o*-xylene reasonable solar cells are made with a PCE of 3.2%, but even after extensive optimization this could not be significantly increased. Even more striking is that when toluene or *m*-xylene were used to deposit [70]PCBM the results were even worse, with PCEs of only 0.1% and 0.5% respectively. Optical microscopy (**Figure 5**a,c) and scanning electron microscopy (SEM, Figure 5b,d) reveal that the low efficiency found using toluene or *m*-xylene can be ascribed to a poor film morphology. The images show formation of droplet-like features and dendritic crystallites on top of the polymer film. The latter can only be due to [70]PCBM. By eye, the film in-between the droplets is clearly greener than the redder films made from *o*-xylene and TMB, indicating a low fullerene content in the polymer film. The reduced amount fullerene that is mixed with the polymer explains the strongly reduced photovoltaic performance. With optical microscopy no significant differences can be seen between *o*-xylene and TMB (Figure 5e,f). However, using atomic force microscopy (AFM) a clear difference can be seen. For TMB a very homogeneous film has been formed (Figure 5h), while we see an inhomogeneous surface morphology for *o*-xylene (Figure 5g), which we expect to be caused by deposition of [70]PCBM on top of the polymer-rich film. The resulting gradient in sulfur content has been verified using XPS (see the Supporting Information). The moderate efficiency in the sequentially doctor bladed films from *o*-xylene is thus caused by a quasi-bilayered structure in which the fullerene has insufficiently penetrated into the

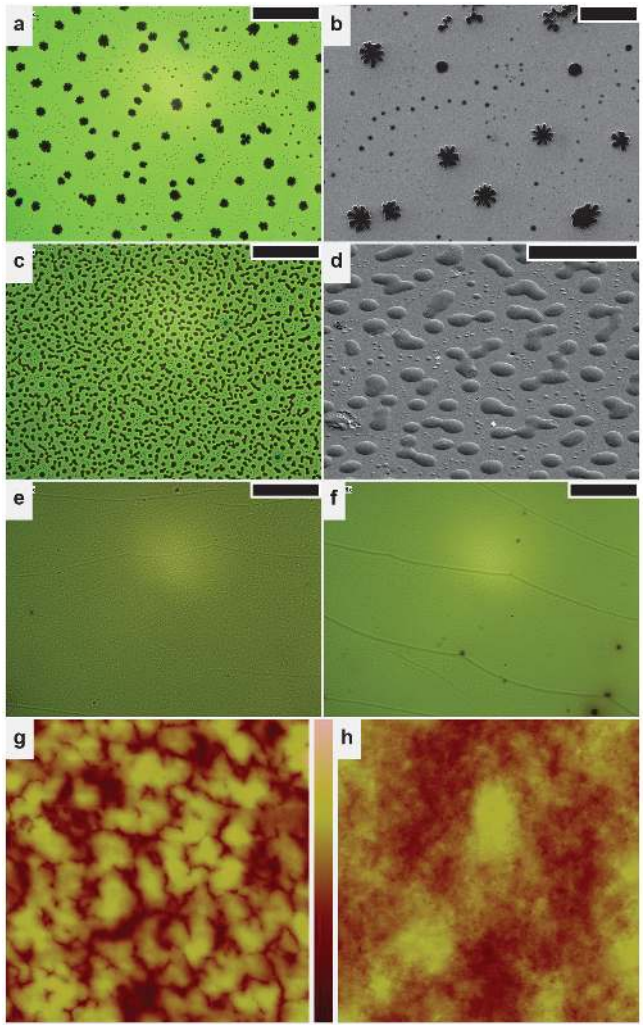

Figure 5. a,c,e,f) Optical images (scale bar 60 µm), b,d) SEM images (scale bar 20 µm), and g,h) AFM height images (lateral scale 5.0 µm, height scale 40 nm) of sequentially processed solar cells, using a,b) toluene, c,d) *m*-xylene, e,g) *o*-xylene, and f,h) TMB as second-layer solvents. The lines in (e,f) are caused by the movement of the drying front during doctor blade coating.

polymer film, and the remainder has been deposited on top of the polymer-rich film, similar to the solar cells made by sequential spin coating of [70]PCBM from *o*-xylene (Figure 3). The differences in the exact morphology of the [70]PCBM deposited on top of the polymer-rich layer between the doctor bladed sample (Figure 5g) and the spin coated sample (Figure 3) can be well explained by the differences in coating method and coating temperature.

2.5. Polymer Swelling in the Second-Layer Solvent

To make efficient solar cells, [70]PCBM has to infiltrate the polymer layer during processing from a second solvent. This can be achieved if this second-layer solvent swells the polymer film, thereby enabling the fullerene to infiltrate into the polymer film. A possible cause for bad performing sequentially processed solar cells is that the second-layer solvent is unable to swell the polymer layer sufficiently. To measure the extent of polymer swelling in different solvents, we used a quartz crystal microbalance with dissipation (QCM-d).[16] In this experiment, a quartz crystal is brought into oscillation at its resonance frequency. If mass is added to the crystal and joins the oscillating movement, the resonance frequency will change. The details of this measurement method are explained in Section 4, Supporting Information.

To study polymer swelling a quartz crystal is coated with a PDPP5T film (thickness 40–50 nm). Solvents are then flowed over the polymer-coated side of the quartz crystal in a flow-cell geometry. A typical measurement sequence is shown in **Figure 6**a. First, as a nonsolvent, 2-propanol (IPA) is flowed over the PDPP5T layer. IPA does not increase the measured mass density: as expected the polymer film is not swollen by IPA. After that the test-solvent (*o*-xylene in the example shown in Figure 6a), is flowed over the PDPP5T. This increases the mass density measured by the QCM-d, indicating that *o*-xylene swells the polymer film and the mass of the solvent that has infiltrated the polymer layer joins the oscillation of the quartz crystal. This mass density increase can be converted into a thickness increase using the density of the solvent, because all added mass is solvent. When IPA is flowed again, the film mass density does not decrease to an entirely unswollen state, either because not all *o*-xylene can be removed from the film, or because IPA cannot swell PDPP5T by itself but may infiltrate the space made by *o*-xylene. Then the polymer film is blow-dried by air and it can be seen that the mass density is slightly negative: the flow of o-xylene has removed a small part of the polymer film. After this again IPA is used, but now it seems that even this nonsolvent causes a (small) mass density increase. This might be explained by the fact that the film is now rougher or more porous, and thus some IPA joins the oscillation at the surface. A repeated flow of *o*-xylene and IPA shows the swelling is reproducible. Then a good solvent (CF) is flowed, which first shortly increases the mass density (indicating large swelling) and then decreases the mass density (indicating removal of the film). Now the crystal is further washed with *o*-xylene and IPA before blow-drying again with air. The total mass density that has been removed by CF can then be converted into the initial polymer layer thickness using

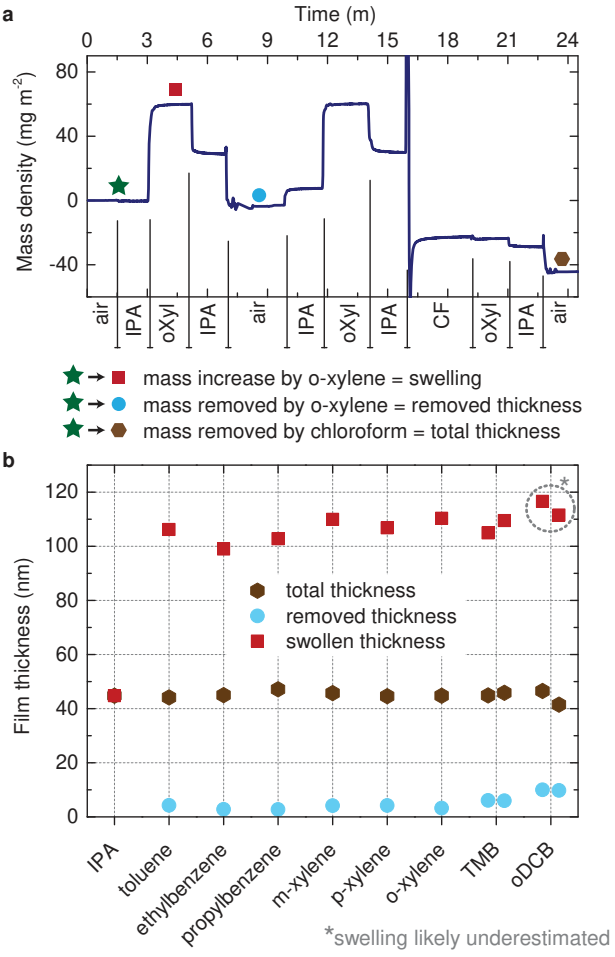

Figure 6. Polymer swelling measurements with a quartz crystal microbalance. In panel (a) a measurement for *o*-xylene is shown, which is typical for all nonhalogenated aromatic solvents. A quartz crystal is coated with a 40–50 nm polymer layer, and then mounted in the setup. Then various solvents are flowed in sequence over the coated side of the crystal. A nonsolvent (IPA) causes no increase of mass density on the sensor, thus no swelling, whereas partial solvents do cause an increase of mass density and thus swelling. The sensor is blow-dried with air to measure the mass removed by the partial solvent. Finally, a good solvent (CF) is used to remove the remaining polymer film from the quartz crystal. In panel (b) the results are summarized for all solvents tested. These indicate that swelling is very similar for all non-halogenated aromatic solvents. For oDCB the swelling seems similar as well, but as discussed in Section 4, Supporting Information, this measurement is likely underestimated. The measurement for TMB and oDCB has been performed in duplicate to verify reproducibility.

the estimated density of PDPP5T (1000 kg m^{-3}). The small steps from *o*-xylene–IPA–air are not totally understood, but might be related to small amounts of remaining polymer or droplet formation on the crystal surface.

To investigate if limited swelling can explain the differences in performance of sequentially processed solar cells these experiments have been performed on a series of aromatic solvents. The data is shown in Figure 6b. First, to check if the thicknesses as measured by the QCM-d are reliable, the total thickness as measured by the QCM-d (40–45 nm) is compared to film thicknesses measured with a profilometer (40–50 nm). This

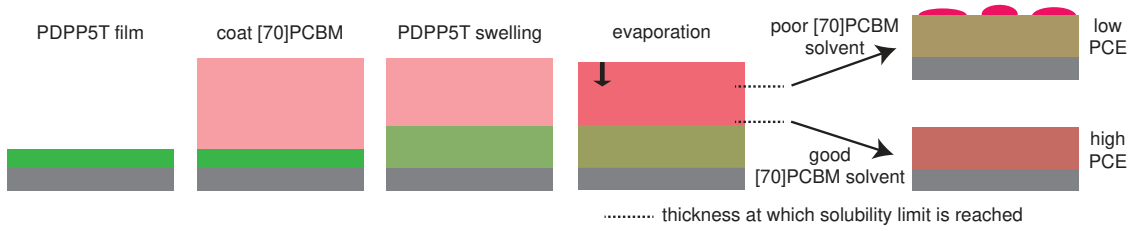

Figure 7. Schematic steps in sequential processing. A low [70]PCBM solubility in the second-layer solvent causes the formation of droplet-like features and dendritic crystallites on top of the polymer film and a too-low mixing ratio of the fullerene in the polymer film, which severely hinders the solar cell efficiency.

good correspondence indicates that the QCM-d measurement is reliable. Second, regarding polymer swelling all non-halogenated aromatic solvents behave similarly, with a thickness increase of 118%–141%. This indicates that differences in swelling are not responsible for the trends in solar cell performance. For oDCB the swelling seems only slightly higher than for the nonhalogenated solvents, but this is likely to be underestimated (see Section 4, Supporting Information). Finally, the removed thickness is very similar for all nonhalogenated solvents because less than 10% of the initial polymer film is removed by these solvents, except for TMB where ≈15% of the film is removed. For oDCB ≈23% of the film is removed. This might indicate that an increased amount of removed material is beneficial for solar cell performance. However, because the space made by removed material is small compared to the space made by polymer swelling we believe this is not the primary reason for the success of second-layer solvents.

2.6. Evaporation Rate of the Second-Layer Solvent

In Section 2.5 we have shown that the swelling of the PDPP5T film is similar in toluene and TMB. However, when TMB is used as second-layer solvent in sequentially processed solar cells, efficiencies of up to 5.3% are reached, while efficiencies are limited to 0.1% when using toluene (Figure 4, Table 2). The limited efficiency for solar cells made using toluene is clearly caused by the formation of droplet-like features and dendritic crystallites of [70]PCBM on top of the polymer film (Figure 5). A significant difference between TMB and toluene is their evaporation rate. The boiling point of TMB is 169 °C, while that of toluene is only 110 °C.[14] It might be that due to the faster evaporation of toluene the fullerene has insufficient time to infiltrate the PDPP5T layer, which would then cause the low efficiency. To clarify the influence of solvent evaporation rate, solar cells were made using toluene, ethylbenzene, and *n*-propylbenzene. The increasing length of the alkyl chain increases the boiling point (Table 2) and decreases the evaporation rate. As shown in Table 2, there is a trend that the PCE increases with boiling point, up to 0.3% for *n*-propylbenzene. However, these PCEs are very low compared to those obtained with TMB, even though the boiling point of *n*-propylbenzene (159 °C) is very close to that of TMB (169 °C). Thus, the fast evaporation rate of toluene is not the cause of the low efficiency. The formation of droplet-like features and dendritic crystallites which occurs for toluene does also occur for ethylbenzene and *n*-propylbenzene (not shown) and explains these low efficiencies.

2.7. Solubility of [70]PCBM in the Second-Layer Solvent

Crystallization on top of the polymer film might be caused by a low solubility of the [70]PCBM in the second-layer solvent. To test this possibility the solubility of [70]PCBM was measured for all non-chlorinated solvents (and solvent combinations) and the results are collected in Table 2. The [70]PCBM solubility in oDCB was taken from literature.[15] Table 2 clearly shows that high-performing solar cells can only be made with solvents in which [70]PCBM is highly soluble. This provides a qualitative understanding of sequential processing as shown schematically in **Figure 7**. For all non-halogenated aromatic solvents collected in Table 2 the PDPP5T film will initially swell to a similar extent, creating a bilayer of a polymer layer infiltrated with the [70]PCBM solution and a [70]PCBM solution on top of the swollen polymer. During subsequent evaporation of the solvent, the solubility limit of [70]PCBM will be reached at some point in time. At this moment the [70]PCBM which has already infiltrated the polymer film will be remain in the film and determine the mixing ratio in the polymer-rich film. The [70]PCBM present

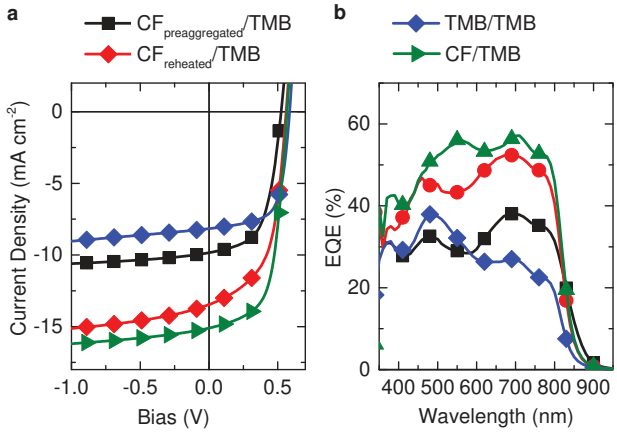

Figure 8. a) *J*–*V* and b) EQE measurements of sequentially processed solar cells, in which the (first) polymer layer was spin coated from either a fresh solution in CF, from an aged solution in CF (preaggregated) and from the same solution but then reheated to remove the aggregates (reheated). Also a solar cell processed entirely from nonhalogenated aromatic solvents is shown, where the polymer (PDPP5T) was spin coated from a hot solution in TMB. [70]PCBM was always doctor bladed from TMB.

in the remaining solvent layer on top of the polymer film will be deposited there, either in the form of crystallites (toluene), amorphous droplet-like domains (most xylenes), or a quasi-bilayered structure (*o*-xylene).

The remaining question then is why TMB and oDCB sequentially processed cells can form a well-mixed vertical distribution of [70]PCBM and PDPP5T which leads to high-performing solar cells, while those made from *o*-xylene do not form this correct vertical composition profile and thus suffer in photovoltaic performance. How can we explain this difference, even though the measured solubility for [70]PCBM is similar? For oDCB this can be explained by the swelling, which is likely to be more than for the non-halogenated solvents (Section 4, Supporting Information). With a similar solubility for [70]PCBM more fullerene can infiltrate the more swollen layer, because at the moment the solubility limit is reached more fullerene is inside the swollen polymer film. The difference between *o*-xylene and TMB is not well understood. It might be that the solubility of [70]PCBM in TMB is higher than in *o*-xylene, which could not be measured due to the already high solubility of [70]PCBM in both solvents. A hint that this might be the case is that the reported solubility of C60 in TMB is 17.9 mg mL^{-1}, which more than twice that for *o*-xylene (8.7 mg mL^{-1}).[17]

2.8. Influence of the Polymer Layer Morphology

Now that we understand the influence of important parameters of the second-layer solvent, it remains of interest to study if there is any influence of the morphology of the first layer. It would be beneficial if we could separate polymer deposition from the final morphology formation, such that the morphology would solely be determined during the processing of the second layer. If this would be the case, the polymer layer might be deposited at higher temperatures from non-halogenated solvents, without having to worry about the formed morphology.

To test the effect of the deposition method of the first layer, a solution of PDPP5T in CF was left to age at room temperature. During ageing of this polymer small aggregates are formed, as evidenced from a significant red-shift in the optical absorption. The aggregates remain finely dispersed in the solution.[18] This 2 month old "preaggregated" solution was spin coated as usual. On top of this preaggregated PDPP5T layer, [70]PCBM has been doctor bladed from TMB. The PCE of 3.0% is significantly lower than that of the reference CF/TMB device (Table 2, PCE = 5.3%) and than that of a cell made with a polymer layer from the aged solution after reheating (20 min at 90 °C, PCE = 4.2%; **Figure 8**). The cell processed from the preaggregated solution is slightly thicker (137 nm) than the cell processed from the reheated solution (115 nm) due to the higher viscosity of the preaggregated solution. This thickness difference and the resulting change in PDPP5T:[70]PCBM ratio can partly explain the decrease in performance. However, the large difference in PCE clearly indicates that the state of the used polymer solution, and thus the morphology of the polymer layer, is important in the success of sequential processing. In this case the preaggregation decreases the efficiency, maybe because the fullerene is unable to penetrate the crystalline regions of the aggregated polymer.

We also processed solar cells entirely from non-halogenated solvents. To do that a slightly more soluble lower molecular weight (M_p = 38 vs 42 kDa) version of the PDPP5T polymer was used. This version could be dissolved in TMB at 110 °C and then spin coated from this hot solution. Then the [70]PCBM was doctor bladed on top from TMB. A thickness optimization series let to a best PCE of 3.2% (Figure 8). This result shows that it is possible to process PDPP5T:[70]PCBM solar cells entirely from non-halogenated solvents, but that the efficiency is lower than when the first layer is deposited from CF.

Both experiments show that the morphology of the polymer layer is important, and that the first solvent influences the performance too.

3. Conclusion

Efficient polymer:fullerene solar bulk heterojunction solar cells have been made via a sequential processing procedure in which the fullerene is deposited on top of a polymer layer, avoiding the use of solvent/cosolvent mixtures. The efficiency of the procedure is highly dependent on the second-layer solvent used for the fullerene. It was found that all tested non-halogenated aromatic solvents swell the polymer film similarly, but result in a widely different solar cell performance. While polymer swelling is a necessity, the main factor to influence the performance is found to be the solubility of the fullerene in the second-layer solvent. A too low solubility prevents sufficient infiltration of the fullerene in the polymer film, and causes the formation of droplet-like features and dendritic crystallites on top of the polymer film, or a quasi-bilayered structure. The fullerene content in the polymer-rich film is then too low to enable efficient charge transport, which significantly hinders the solar cell efficiency.

Similar to the conventional processing of organic solar cells, the universality of sequential processing depends largely on the availability of suitable solvents for each new polymer:fullerene combination. Recently, the success of this method has been shown for many different material combinations.[10] Because the solvent from which the polymer is deposited does not need to dissolve the fullerene, more options are available for depositing the polymer layer. Furthermore, Aguirre et al. have recently demonstrated an elegant method to meet the dual requirement for the second-layer solvent using a mixture of two solvents to swell the polymer layer and infiltrate the fullerene.[10f] We thus expect that sequential processing will be possible for many polymer:fullerene systems.

Because sequential processing uses single solvents for each component, we expect it can be transferred more easily to roll-to-roll production methods than conventional processing using a solvent/cosolvent mixture. It allows solar cells to be made entirely from non-halogenated solvents, but likely more effort is needed to bring their efficiencies up to par with conventional processing. Without doubt, sequential processing holds promise to be used as an alternative solution-based deposition method to make relevant bulk heterojunction morphologies for organic solar cells.

4. Experimental Section

Basic Solar Cell Preparation: Indium tin oxide (ITO) substrates (30 × 30 mm, Naranjo) were cleaned by sonication with acetone, followed by washing with soap, sonication in soap, deionizing in demineralized water, and sonication in 2-propanol. Then the substrates were exposed to UV-ozone for 30 min. PEDOT:PSS (Heraeus Clevios P VP Al4083) was spin coated at 3000 rpm in air (thickness ≈ 40 nm) as hole extracting electrode. All active layers were also coated in air (see below for exact methods). The electron extracting top electrode, consisting of 1 nm lithium fluoride and 100 nm aluminum, was thermally evaporated in a vacuum chamber at base pressure of less than 10^{-6} mbar through a shadow mask. The active area was determined by the overlap between ITO and aluminum and was either 3 × 3 mm or 4 × 4 mm. The diketopyrrolopyrrole-quinquethiophene polymer (PDPP5T) was supplied by BASF. Two batches were used: batch GSID4133–1 with M_p = 42 kDa, and batch GSID4133–2 with slightly lower M_p of 38 kDa. These M_p values differ from those mentioned in Section 2.1, because these are measured in oDCB at 140 °C. [70]PCBM was obtained from Solenne BV, >90% purity. The used doctor blade equipment was an Erichsen coatmaster 509 MC. A Veeco Dektak 150 was used to measure layer thicknesses.

Fully Spin Coated Cells: For CF only: PDPP5T (6 mg mL^{-1}) and [70]PCBM (12 mg mL^{-1}) were codissolved in CF and stirred overnight at 60 °C. This solution was spin coated on top of the PEDOT:PSS layer at 2000 rpm (thickness 92 nm). For CF:oDCB: PDPP5T (6 mg mL^{-1}) and [70]PCBM (12 mg mL^{-1}) were codissolved in a solvent mixture with 95 vol% CF and 5 vol% oDCB. This solution was stirred overnight at 60 °C and spin coated at 2000 rpm on top of the PEDOT:PSS layer (thickness 81 nm). For CF/oDCB: PDPP5T (6 mg mL^{-1}) was dissolved in CF and stirred overnight at 60 °C and spin coated on the PEDOT:PSS layer between 450 and 1500 rpm to obtain layer thicknesses between 45 and 80 nm. [70]PCBM (24 mg mL^{-1}) was dissolved in oDCB with 15 min of sonication and spin coated on top of the PDPP5T layer, while making sure that the initial drop covered all active areas. Spin coating was done between 600 and 3000 pm to reach final layer thicknesses between 52 and 130 nm of which the PDPP5T:[70]PCBM ratio has been determined as mentioned in the main text. The example cell with PDPP5T:PCBM ratio 1:4 had the PDPP5T layer spin coated at 800 rpm (thickness: 58 nm) and the [70]PCBM layer spin coated at 1500 rpm, resulting in a final layer thickness of 91 nm. For CF/*o*-xylene: PDPP5T (6 mg mL^{-1}) was dissolved in CF and stirred overnight at 60 °C and spin coated on the PEDOT:PSS layer at 800 rpm. [70]PCBM (20 mg mL^{-1}) was dissolved in *o*-xylene with 15 min of sonication and spin coated on top of the PDPP5T layer at 800 rpm. Final thickness was 90 nm.

Doctor Bladed Reference CF:oDCB: PDPP5T (6 mg mL^{-1}) and [70]PCBM (12 mg mL^{-1}) were codissolved in a solvent mixture with 95 vol% CF and 5 vol% oDCB. This solution was stirred for 1 h at 90 °C and then coated using a blade height of 254 µm, a blade speed of 40 mm s^{-1}, a coating temperature of 50 °C and a liquid volume of 60 µL. The layer thickness was 114 nm.

Doctor Bladed [70]PCBM Cells: PDPP5T (6 mg mL^{-1}) was dissolved in chloroform by stirring 1 h at 90 °C. This solution was spin coated at 1250 rpm which resulted in a layer thickness of 40–50 nm. Then [70]PCBM was dissolved (20 mg mL^{-1} for halogen-free solvents, 10 mg mL^{-1} for oDCB) by 15 min of sonication. These solutions were doctor bladed on top of the PDPP5T layer using a blade height of 254 µm, a blade speed of 20 mm s^{-1}, a coating temperature of 50 °C and a liquid volume of 50 µL for halogen-free solvents and 20 µL for oDCB. Thicknesses were typically 100–120 nm for the uniform films.

Nonhalogenated TMB/TMB Device: PDPP5T-2 (8 mg mL^{-1}) was dissolved in TMB by stirring at 110 °C for 1 h. This solution was spin coated hot at 2400 rpm (thickness ≈ 50 nm). [70]PCBM was doctor bladed from a 20 mg mL^{-1} solution in TMB at 50 °C, using a blade height of 254 µm, a blade speed of 20 mm s^{-1} and a droplet volume of 15 µL. The total thickness was 83 nm.

Current Density–Voltage Measurements: Current density–voltage (*J–V*) curves were measured in nitrogen under simulated sunlight conditions from a tungsten halogen-lamp setup with a Schott GG385 UV-filter and a Hoya LB120 daylight filter. The system was calibrated with a Si reference cell to obtain an intensity of 100 mW cm^{-2}. A voltage sweep from −2 to +2 V was done using a Keithley 2400 source meter.

External Quantum Efficiency: EQE was determined using a 50 W Philips focusline tungsten halogen lamp in combination with an Oriel Cornerstone 130 monochromator. The signal was amplified by a Stanford Research System Model SR570 and then measured by a lock-in amplifier (Stanford Research Systems SR830). These measurements were converted to EQE by comparing the measurement with a silicon reference cell.

[70]PCBM Solubility Measurements: At least 30 mg of [70]PCBM was dissolved in 0.3 mL of the solvents given in Table 1 by sonicating for 15 min. If there was no solid [70]PCBM remaining after this more [70]PCBM was added and again sonicated. This was repeated until the added [70]PCBM did not dissolve. In the case of *o*-xylene and TMB this was hard to judge due to the high viscosity of the solutions. The saturated solutions were left overnight and then filtered through a 0.22 µm PTFE filter and then diluted by at least a factor 100 to be able to measure the absorption. The solubility was calculated by fitting to the average absorption of four reference solutions of 0.06–0.48 mg mL^{-1} [70]PCBM in toluene and then multiplying by the dilution factor.

Other Characterization: TEM images were obtained on a FEI Tecnai G2 200 kV using a LaB_6 filament. Magnification was 14500× resulting in 1.21 × 1.21 µm pictured areas. Defocus was set to −9 µm. The SEM-image (Figure 5b) was taken on a JEOL JSM-5600. The SEM-image (Figure 5d) was taken under a 52° angle on a FEI Quanta 3D FEG. UV–vis absorption measurements were done on a Perkin Elmer Lambda 900. AFM was done using Nanosensor PPP-NCHR-50 tips, in tapping mode on a Veeco Multimode AFM.

Supporting Information

Supporting Information is available from the Wiley Online Library or from the author.

Acknowledgements

This research forms part of the research program of the Dutch Polymer Institute (DPI), Project No. 734. The authors thank Bardo Bruijnaers and Fallon Colberts for the SEM-images and thank Chen Meng for his preliminary work on doctor bladed, sequentially processed solar cells. The authors also acknowledge Tiny Verhoeven for additional XPS measurements and thank Olga Goor and Bram Pape for their help with the QCM-d measurements. The research is part of the Solliance OPV program and has received funding from the Ministry of Education, Culture and Science (Gravity 382 program 024.001.035).

Received: March 5, 2015
Revised: April 22, 2015
Published online: May 15, 2015

[1] Y. Liu, J. Zhao, Z. Li, C. Mu, W. Ma, H. Hu, K. Jiang, H. Lin, H. Ade, H. Yan, *Nat. Commun.* **2014**, *5*, 5293.
[2] N. Grossiord, J. M. Kroon, R. Andriessen, P. W. M. Blom, *Org. Electron.* **2012**, *13*, 432.
[3] R. Søndergaard, M. Hösel, D. Angmo, T. T. Larsen-Olsen, F. C. Krebs, *Mater. Today* **2012**, *15*, 36.
[4] a) J. K. Lee, W. L. Ma, C. J. Brabec, J. Yuen, J. S. Moon, J. Y. Kim, K. Lee, G. C. Bazan, A. J. Heeger, *J. Am. Chem. Soc.* **2008**, *130*, 3619; b) L. Dou, J. You, Z. Hong, Z. Xu, G. Li, R. A. Street, Y. Yang, *Adv. Mater.* **2013**, *25*, 6642.
[5] a) S. S. Ghosh, G. S. Lonkar, M. S. Mahajan, S. R. Jadkar, V. S. Waman, M. M. Kamble, V. Ganesan, J. V. Sali, *Appl. Phys.*

Lett. **2012**, *101*, 173305; b) B. Schmidt-Hansberg, M. Sanyal, M. F. G. Klein, M. Pfaff, N. Schnabel, S. Jaiser, A. Vorobiev, E. Müller, A. Colsmann, P. Scharfer, D. Gerthsen, U. Lemmer, E. Barrena, W. Schabel, *ACS Nano* **2011**, *5*, 8579.

[6] S. Kouijzer, J. J. Michels, M. van den Berg, V. S. Gevaerts, M. Turbiez, M. M. Wienk, R. A. J. Janssen, *J. Am. Chem. Soc.* **2013**, *135*, 12057.

[7] a) J. J. M. Halls, C. A. Walsh, N. C. Greenham, E. A. Marseglia, R. H. Friend, S. C. Moratti, A. B. Holmes, *Nature* **1995**, *376*, 498; b) G. Yu, J. Gao, J. C. Hummelen, F. Wudl, A. J. Heeger, *Science* **1995**, *270*, 1789.

[8] a) A. L. Ayzner, C. J. Tassone, S. H. Tolbert, B. J. Schwartz, *J. Phys. Chem. C* **2009**, *113*, 20050; b) V. S. Gevaerts, L. J. A. Koster, M. M. Wienk, R. A. J. Janssen, *ACS Appl. Mater. Interfaces* **2011**, *3*, 3252.

[9] B. Liu, R.-Q. Png, L.-H. Zhao, L.-L. Chua, R. H. Friend, P. K. H. Ho, *Nat. Commun.* **2012**, *3*, 1321.

[10] a) D. H. Wang, J. S. Moon, J. Seifter, J. Jo, J. H. Park, O. O. Park, A. J. Heeger, *Nano Lett.* **2011**, *11*, 3163; b) D. H. Kim, J. Mei, A. L. Ayzner, K. Schmidt, G. Giri, A. L. Appleton, M. F. Toney, Z. Bao, *Energy Environ. Sci.* **2014**, *7*, 1103; c) P. Cheng, J. Hou, Y. Li, X. Zhan, *Adv. Energy Mater.* **2014**, *4*, 1301349; d) Y. Liu, H.-W. Wang, D. Nordlund, Z. Sun, S. Ferdous, T. P. Russell, *ACS Appl. Mater. Interfaces* **2015**, *7*, 663; e) J. Seok, T. J. Shin, S. Park, C. Cho, J.-Y. Lee, D. Y. Ryu, M. H. Kim, K. Kim, *Sci. Rep.* **2015**, *5*, 8373; f) J. C. Aguirre, S. A. Hawks, A. S. Ferreira, P. Yee, S. Subramaniyan, S. A. Jenekhe, S. H. Tolbert, B. J. Schwartz, *Adv. Energy Mater.* **2015**, DOI: 10.1002/aenm.201402020.

[11] S. A. Hawks, J. C. Aguirre, L. T. Schelhas, R. J. Thompson, R. C. Huber, A. S. Ferreira, G. Zhang, A. A. Herzing, S. H. Tolbert, B. J. Schwartz, *J. Phys. Chem. C.* **2014**, *118*, 17413.

[12] M. Campoy-Quiles, T. Ferenczi, T. Agostinelli, P. G. Etchegoin, Y. Kim, T. D. Anthopoulos, P. N. Stavrinou, D. D. C. Bradley, J. Nelson, *Nat. Mater.* **2008**, *7*, 158.

[13] N. Li, D. Baran, K. Forberich, M. Turbiez, T. Ameri, F. C. Krebs, C. J. Brabec, *Adv. Energy Mater.* **2013**, *3*, 1597.

[14] W. M. Haynes, *CRC Handbook of Chemistry and Physics*, 95th ed., CRC Press, London **2014**, pp. 6–88.

[15] D. T. Duong, B. Walker, J. Lin, C. Kim, J. Love, B. Purushothaman, J. E. Anthony, T.-Q. Nguyen, *J. Polym. Sci. B: Polym. Phys.* **2012**, *50*, 1405.

[16] a) I. Reviakine, D. Johannsmann, R. P. Richter, *Anal. Chem.* **2011**, *83*, 8838; b) Z. Parlak, C. Biet, S. Zauscher, *Meas. Sci. Technol.* **2013**, *24*, 85301; c) G. Sauerbrey, *Z. Physik.* **1959**, *155*, 206.

[17] W. A. Scrivens, J. M. Tour, *J. Chem. Soc., Chem. Commun.* **1993**, *15*, 1207.

[18] J. J. van Franeker, M. Turbiez, W. Li, M. M. Wienk, R. A. J. Janssen, *Nat. Commun.* **2015**, *6*, 6229.